Journal of Power Sources 215 (2012) 216–220

Contents lists available at SciVerse ScienceDirect

Journal of Power Sources

journal homepage: www.elsevier.com/locate/jpowsour

Short communication

Nitrogen-doped carbon nanotubes as catalysts for oxygen reduction reaction

Chun Xiong, Zidong Wei*, Baoshan Hu, Siguo Chen, Li Li, Lin Guo, Wei Ding, Xiao Liu, Weijia Ji, Xiaopei Wang

State Key Laboratory of Power Transmission Equipment & System Security and New Technology, School of Chemistry and Chemical Engineering, Chongqing University, Chongqing 400030, China

HIGHLIGHTS

- The aligned nitrogen-doped carbon nanotubes (NCNT) were synthesized.
- NCNT doped from melamine and urea was named M-NCNT and U-NCNT, respectively.
- M-NCNT has higher nitrogen content and more defects than U-NCNT.
- M-NCNT has shown better ORR performance than U-NCNT.

ARTICLE INFO

Article history:
Received 10 March 2012
Received in revised form
19 April 2012
Accepted 20 April 2012
Available online 8 May 2012

Keywords:
Nitrogen-doped
Carbon nanotubes
Oxygen reduction reaction
Electrocatalysis

ABSTRACT

The aligned nitrogen-doped carbon nanotubes (NCNT) with bamboo-like structure are synthesized via thermal chemical vapor deposition using melamine and urea as different nitrogen precursors. Meanwhile, ferrocene is used as catalyst and carbon precursor. The resulting NCNT with melamine (M-NCNT) have shown superior ORR performance in terms of limiting current density and number of electrons transferred. Further characterizations by X-ray photoelectron spectroscopy (XPS) and Raman spectroscopy illustrated higher nitrogen content and more defects in M-NCNT compared to that in NCNT with urea (U-NCNT), which indicate the important role of the nitrogen precursor in nitrogen content and structure of NCNT. It is concluded that higher nitrogen content and more defects of NCNT lead to high performance of ORR.

1. Introduction

The oxygen reduction reaction (ORR) is one of the most crucial factors determining the performance of a fuel cell [1]. Highly active catalysts for ORR are essential to optimize the performance of fuel cells because of the kinetic sluggishness of ORR [2–5]. Platinum-based materials have long been investigated as active catalysts for ORR [6–10], nevertheless, this noble metal catalyst and its alloy can hardly meet the demands for widespread commercialization of fuel cells because of their sluggish electron transfer kinetics [11], high costs, limited supply [12], and poor durability [13]. Thus, nonprecious-metal [14,15] and metal-free catalysts [4,5,16–18] for ORR have attracted enormous interest as an alternative to platinum-based catalysts.

Recently, nitrogen-doped carbon nanotubes (NCNT) have been demonstrated to show excellent electrocatalytic activities for ORR [4,5] because of their unique electronic properties originated from the conjugation between the lone-pair electrons of nitrogen and π electron system of the graphene [19]. Generally, NCNT can be prepared by thermal chemical vapor deposition (CVD) of nitrogen-containing precursors [4,5,16,20]. However such a CVD method has still suffered from some challenge so far. For example, high flow rates of carrier gases (more than 8000 sccm) will give rise to uncontrollable structure and unacceptable cost of NCNT [21,22]; while, in the case of low flow rates of carrier gases, the liquid carbon/nitrogen precursors can not be fully evaporated, leaving behind metallocene residues [16,23]. In addition, when the gaseous carbon/nitrogen precursors were used, the valves and connections with quartz tube furnace could be seriously corroded [24]. Meanwhile, toxic amine precursors contained in the off-gas can pollute environment.

This paper reports a modified thermal chemical vapor deposition method with two heating zones to grow aligned NCNT. Melamine (M) and urea (U) as different nitrogen precursors, and ferrocene (F) as carbon precursor and catalyst are placed in the low heating zone. Meanwhile, in the high heating zone, a quartz boat is

* Corresponding author. Tel./fax: +86 23 65106151.
E-mail address: zdwei@cqu.edu.cn (Z. Wei).

0378-7753/$ – see front matter © 2012 Elsevier B.V. All rights reserved.
doi:10.1016/j.jpowsour.2012.04.057

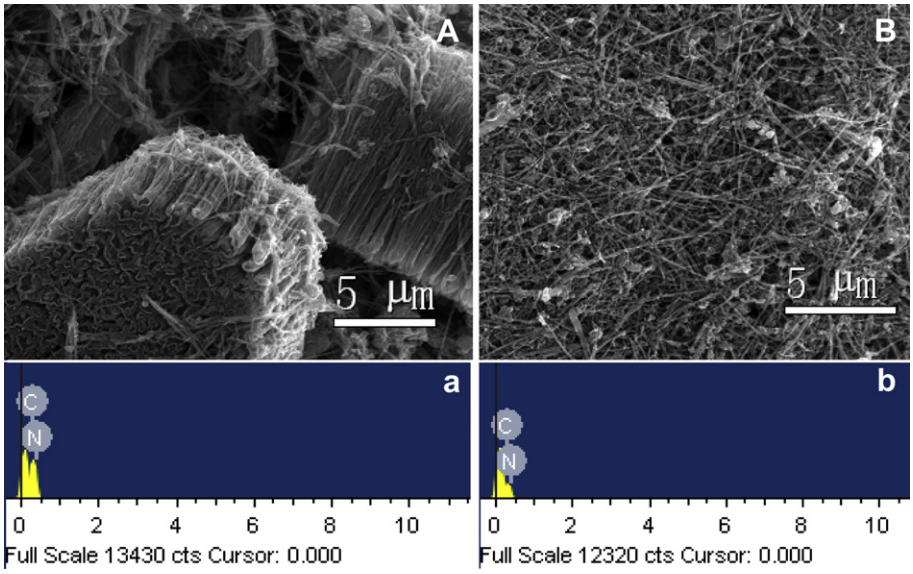

Fig. 1. SEM images of (A) M-NCNT and (B) U-NCNT, EDX spectra of (a) M-NCNT and (b) U-NCNT.

put to collect the NCNT products. The difference in the ORR activity between NCNT grown from F/M mixture (M-NCNT) and F/U mixture (U-NCNT) will be discussed. Furthermore, the effects of different nitrogen precursors on the nitrogen content and the ORR electrocatalytic activity of NCNT will be investigated by comparing M-NCNT and U-NCNT.

2. Experimental methods

2.1. Synthesis of NCNT

NCNT were grown by a modified thermal chemical vapor deposition method. Melamine (M) or urea (U) as solid nitrogen precursor, and ferrocene (F) as carbon precursor and catalyst were placed in the low heating zone, where the temperature was hold at about 400 °C greater than the boiling point of both precursors to ensure full evaporation of the precursors. In the high heating zone, where the temperature was kept at 800 °C, a quartz boat was put to collect the NCNT products. The whole quartz tube furnace was protected by N_2 (99.99%) at a flux of about 50 sccm. The low flow rate of carrier gas can make the precursors fully react in the high heating zone and prevent precursors from wasting. Furthermore, corrosion to quartz tube furnace and pollution of off-gas can be avoided with this method. It is important that the preparation cost of NCNT production is acceptable. Finally, the products were purified by boiling it in nitric acid for 5 h and were dried at 60 °C in a vacuum oven overnight.

2.2. Characterization of NCNT

The morphologies of the NCNT were examined using EDX (FEI Nova 400), a scanning electron microscope (SEM) (FEI Nova 400, Peabody, MA), and a transmission electron microscope (TEM) (Philips TECNAI-20). X-ray photoelectron spectroscopy (XPS, British, Kratos Ltd. XSAM800) was used to investigate the relative content of different elements and the intensity of different nitrogen groups in the NCNT. Raman spectroscopy was used to provide information on the degree of structural defect of NCNT.

2.3. Electrocatalytic activity evaluation of NCNT

Electrochemical measurements were carried out using an Autolab potentiostat/galvanostat (Model, PGSTAT-30, Ecochemie, Brinkman Instruments) in a three-electrode, i.e., Pt wire as

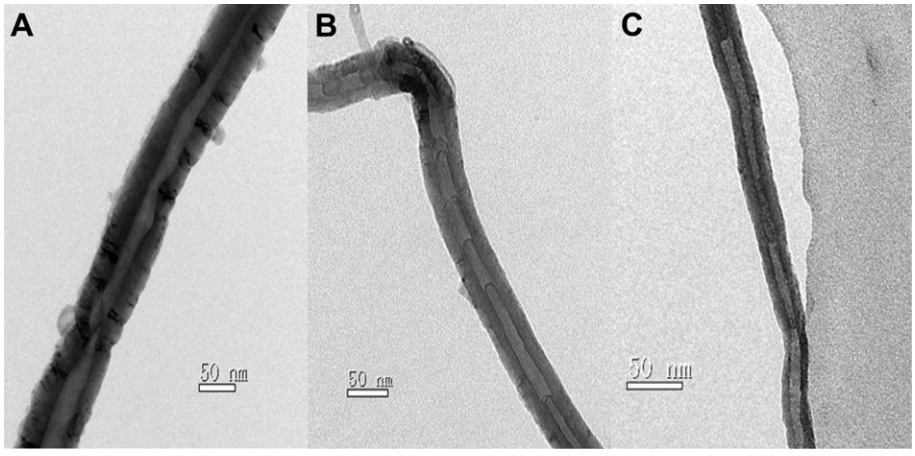

Fig. 2. TEM images of (A) CNTs, (B) M-NCNT and (C) U-NCNT.

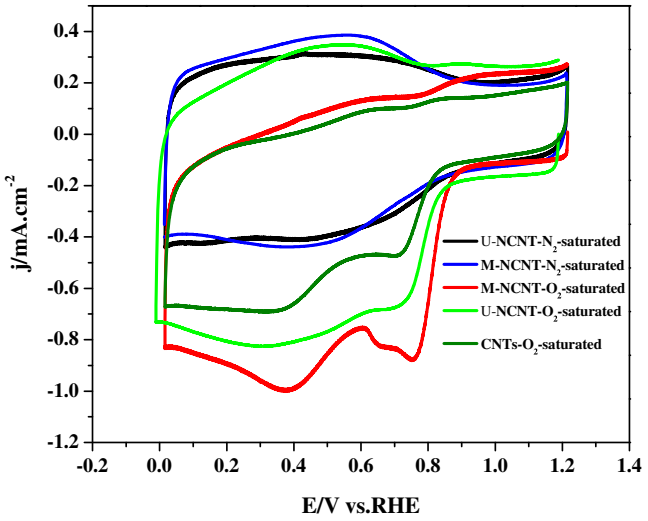

Fig. 3. Cyclic voltammograms on M-NCNT/CG, U-NCNT and CNTs/CG rotating-disk electrodes in 0.1 M KOH solution saturated with N_2 or O_2.

a counter electrode, a reversible hydrogen electrode (RHE) as a reference electrode, and NCNT as a working electrode.

3. Results and discussion

3.1. SEM and TEM analysts

The morphology of M-NCNT and U-NCNT are investigated by means of scanning electron microscopy (SEM). As indicated in Fig. 1, aligned nanotubes can be clearly seen in the cluster of M-NCNT (Fig. 1A), but the morphology of U-NCNT (Fig. 1B) is unordered. Energy dispersive X-ray spectroscopy (EDX) was performed simultaneously with SEM imaging to ensure the major element types of M-NCNT and U-NCNT. EDX analysis shows that nitrogen has been doped into nanotubes (Fig. 1a and b). A more detailed study on the nitrogen content and its bonding with the native carbon atoms by X-ray photoelectron spectroscopy (XPS) will be presented later.

The structure of NCNT is observed by transmission electron microscopy (TEM), which shows bamboo-like structures for M-NCNT (Fig. 2B) and U-NCNT (Fig. 2C). Fig. 2A shows TEM images of pure CNTs which were also fabricated with the above mentioned method without participation of nitrogen precursor. It is typical of the nitrogen-doped nanotubes to have bamboo-like structure in TEM images [5,25]. Thus, TEM images in Fig. 2B and C also prove that nitrogen has been successfully doped into the structure of nanotubes. Differently, M-NCNT have more obvious bamboo-like structures than U-NCNT. It can be explained by the fact that more nitrogen content results in more bamboo-like structures.

3.2. ORR activities of NCNT in alkaline solution

To investigate the electrocatalytic activity of NCNT for the ORR, we compared the electrocatalytic properties of N-doped nanotubes materials (M-NCNT/GC and U-NCNT/GC), and the non-nitrogen nanotubes (CNTs/GC) by cyclic voltammetry in an aqueous solution of nitrogen-protected or O_2-saturated, 0.1 M KOH solution at a scanning rate of 50 mV s^{-1}. As shown in Fig. 3, featureless voltammetric currents on the NCNT/GC in a potential rang of 0 ~ +1.2 V were observed for both M-NCNT and U-NCNT in the N_2-

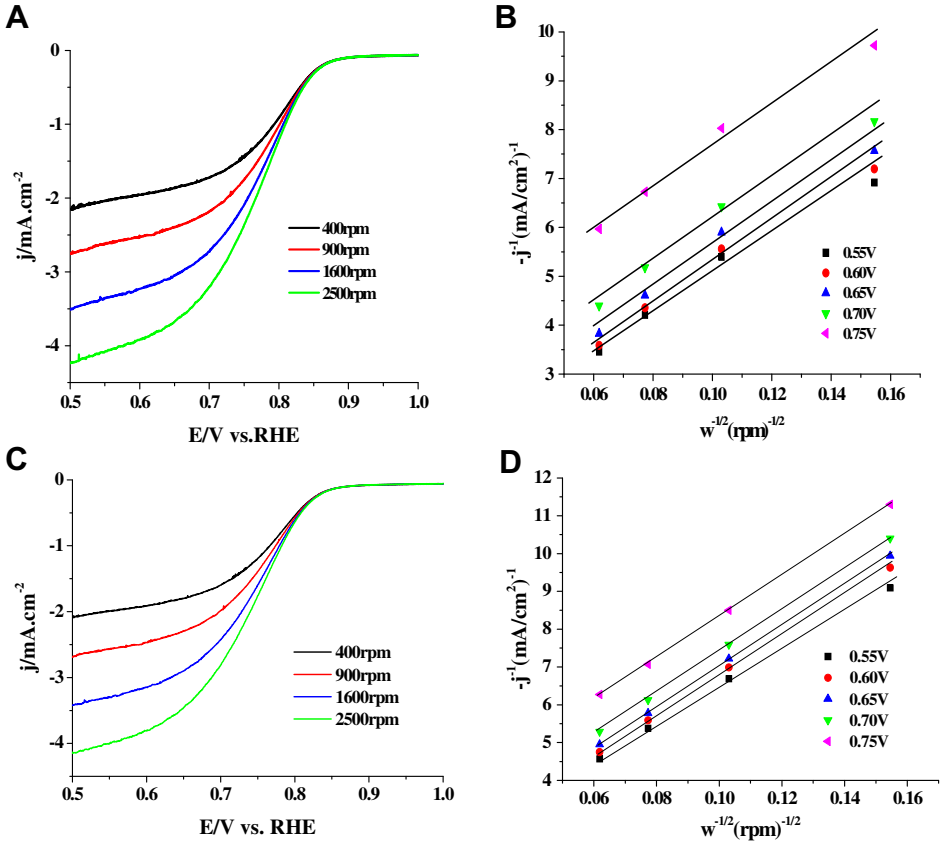

Fig. 4. Rotating-disk voltammograms recorded for (A) M-NCNT/GC and (C) U-NCNT/GC in an O_2-saturated 0.1 M of KOH solution at a scan rate of 10 mV s^{-1}. Koutecky–Levich plots of (B) M-NCNT and (D) U-NCNT.

saturated solution (black curve and blue curve); on the contrary, in the O_2-saturated solution, the reduction current appeared at 0.76 V on the M-NCNT/GC (red curve), and 0.72 V on the U-NCNT/GC (green cure). And the M-NCNT/GC has shown superior ORR performance in terms of limiting current density. It can also be explained by the fact that more nitrogen content (according to XPS) results in superior ORR performance in terms of limiting current density. And except for oxygen reduction peaks, there were multiple peaks in the cathodic scan, which can be ascribed to the impurity absorbed on the electrode. In comparison with M-NCNT/GC, U-NCNT/GC and CNTs/GC, the electrocatalytic activity for ORR is only observed for the NCNT. It means that the doping of nitrogen activates the CNTs for ORR, indicating a promising approach to develop a metal-free catalyst for ORR which can effectively reduce the cost.

To further determine the activity of NCNT for ORR, we investigated the reaction kinetics by rotating-disk voltammetry. The rotating-disk voltammetric profiles in O_2-saturated 0.1 M KOH shown in Fig. 4A–D illustrate that the onset potentials of ORR are approximately 0.88 V for M-NCNT/GC and 0.83 V for U-NCNT/GC, respectively. The kinetic parameters based on Koutecky–Levich plots ($-j^{-1}$ vs.$\omega^{-1/2}$) can be obtained through the following Koutecky–Levich equations [12].

$$\frac{1}{j} = \frac{1}{j_K} + \frac{1}{j_L} = \frac{1}{j_K} + \frac{1}{B\omega^{1/2}} \quad (1)$$

$$B = 0.62nFC_0(D_0)^{2/3}\nu^{-1/6} \quad (2)$$

$$j_K = nFkC_0 \quad (3)$$

Where, j is the measured current density; j_K is the kinetic-limiting current density; j_L is the diffusion-limiting current density; ω is the angular velocity of the disk ($\omega = 2\pi N$, N is the linear rotation speed); n is the overall number of electrons transferred of ORR; F is the Faraday constant (F = 96485 $Cmol^{-1}$); C_0 is the bulk concentration of O_2; ν is the kinematic viscosity of the electrolyte; k is the electron transfer rate constant. According to Eqs. (1) and (2), the number of electrons transferred (n) and j_K can be gained from the slop and intercept of the Koutecky–Levich plots, respectively. By using the values $C_0 = 2.4 \times 10^{-4} molL^{-1}$, $D_0 = 1.73 \times 10^{-5} cm^2 s^{-1}$, and $\nu = 0.01\ cm^2 s^{-1}$ in 0.1M KOH [26], n was calculated (in Table 1) in a range of 0.60–0.70V. It is clear that the transferred number of electrons of M-NCNT situates between 3.7 and 3.9. However, the transferred number of electrons of U-NCNT situates between 3.2 and 3.4. It reveals that ORR almost proceeds on the M-NCNT/GC through a four–electron transfer process and conducts efficiently when catalyzed by M-NCNT.

3.3. XPS and Raman spectroscopy analysts

The elemental composition and different structural groups of nitrogen in M-NCNT and U-NCNT are obtained using XPS (Figs. 5 and 6). From XPS results, M-NCNT had higher nitrogen content than U-NCNT (Table 2) as was expected, since each melamine molecule contains six nitrogen atoms whereas only two nitrogen atoms are present in each urea molecule. Thus, higher ratio of nitrogen to carbon in the growth environment was achieved during nanotubes synthesis when melamine was used. This result is in agreement with the literature which claimed a positive correlation between nitrogen content in NCNT and the number of nitrogen atoms in the precursor molecules [27].

Table 1
Electron transfer numbers of ORR on M-NCNT/GC and U-NCNT/GC.

Potential(V)	0.60	0.65	0.70
M-NCNT Electron number(n)	3.89	3.75	3.72
U-NCNT Electron number(n)	3.35	3.24	3.26

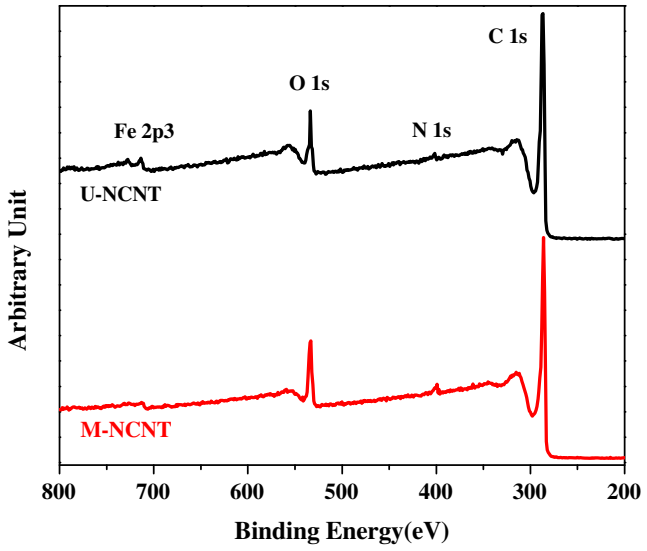

Fig. 5. XPS spectra of M-NCNT and U-NCNT.

It should be noted that oxygen elements were detected in XPS (Fig. 5) but not in the EDX (Fig. 1). This is mainly because that, (1) the depth of XPS scanning is only 3–6 nm, which was used to analysis the surface structure of nanotubes, however, the depth of EDX scanning is micron level (far more than 6 nm), which was used to analysis the whole structure of nanotubes; (2) oxygen is probably doped or absorbed into the surface structure of NCNT while the products were purified by boiling it in nitric acid because there was no oxygen introduction or existence in the whole synthesis of NCNT. Thus, the content of oxygen is too low to be detected by EDX.

From the analysis of the N 1S signal (Fig. 6), peaks centered at 398.27, 400.45, 402.40, and 403.94 eV were observed for M-NCNT. Similar peaks centered at 399.03, 400.22, 402.06, and 404.49 eV

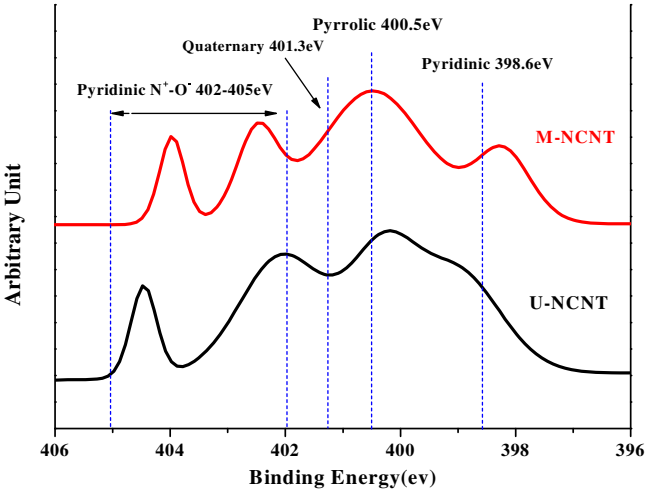

Fig. 6. XPS spectra showing the presence of different types of nitrogen groups from the N 1S signal of M-NCNT (red line) and U-NCNT (black line). (For interpretation of the references to colour in this figure legend, the reader is referred to the web version of this article.)

Table 2
Elemental compositions of M-NCNT and U-NCNT after acid leaching from XPS.

Composition	M-NCNT (at. %)	U-NCNT (at. %)
C	82.84	82.65
N	4.55	2.20
Fe	0.21	0.41
O	12.40	14.74

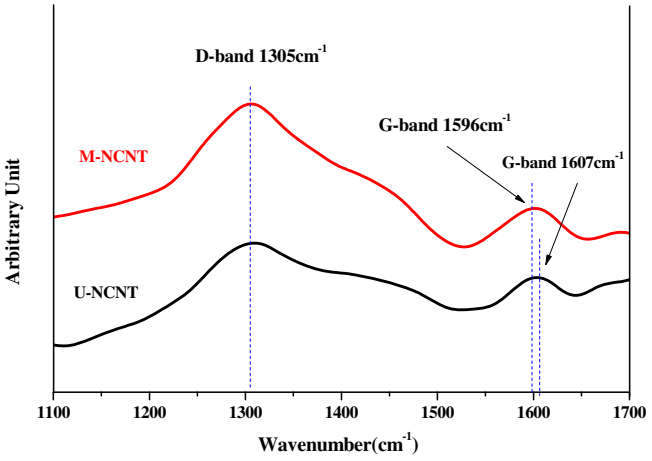

Fig. 7. The Raman spectra of M-NCNT and U-NCNT.

were observed for U-NCNT. The peaks at around 398.27, 400.45, and 402.40–403.94 eV refer to pyridinic nitrogen, pyrrolic nitrogen, and pyridinic N^+–O^- groups in M-NCNT, respectively. Whereas, in the case of U-NCNT, the peaks at around 399.03, 400.22, and 402.06–404.49 eV refer to pyridinic nitrogen, pyrrolic nitrogen and pyridinic N^+–O^- groups, respectively. It is concluded that M-NCNT contains more quaternary nitrogen than U-NCNT as seen in Fig. 6. In addition, since the synthesis of NCNT was carried out under ambient conditions, the reaction between oxygen and nitrogen during synthesis may result in the formation of pyridinic N^+–O^- groups.

Raman spectroscopy was also used to provide information on the degree of structural defect of NCNT (Fig. 7). For M-NCNT, the peak centered at 1305 cm^{-1} is the Raman active D-band and the other centered at 1596 cm^{-1} is the Raman active G-band. The D- and G-bands are also present in U-NCNT centered at 1305 cm^{-1} and 1607 cm^{-1}, respectively. The D-band is ascribed to the finite-sized crystals of graphite, which becomes active because of a reduction in symmetry near or at the crystalline edges [28]. The G-band is due to the E_{2g} vibration mode and is observed in all sp^2 bonds in a graphitic network [28]. The intensity ratio of the D- to G-bands (I_D/I_G) gives qualitative information comparison for the degree of defects in NCNT. A higher I_D/I_G value indicates more defects presented in the nanotubes. From Raman spectra, the I_D/I_G ratios of M-NCNT and U-NCNT are 3.83 and 2.58, respectively, indicating a higher degree of defects in M-NCNT which could be caused by the higher nitrogen content. This conclusion is consistent with the TEM images and XPS data. With respect to U-NCNT, the Raman spectrum of M-NCNT showed a slight downshift of the G-band, possibly caused by the change in electronic structure of NCNT due to the higher nitrogen content [29].

4. Conclusions

In summary, we demonstrated the synthesis of aligned nitrogen-doped carbon nanotubes by a simple and cost-effective approach with two heating steps. M-NCNT show acceptable electrocatalytic activity for oxygen reduction reaction in alkaline solution compared to U-NCNT. ORR almost proceeds on the M-NCNT/GC through a four–electron transfer process efficiently. We also investigated the fundamental roles of nitrogen content and thus-resulted structural defects in NCNT in the ORR activity. It is expected that the aligned NCNT have potential applications in future fuel cells.

Acknowledgements

This work was financially supported by China National 973 Program (2012CB215500 and 2012CB720300) and by NSFC of China (Grant Nos. 20936008 and 21176327).

References

[1] B.C.H. Steele, A. Heinzel, Nature 414 (2001) 345–352.
[2] W. Xiaog, F. Du, Y. Liu, A. Perez Jr., M. Supp, T.S. Ramakrishnan, L.M. Dai, L. Jiang, J. Am. Chem. Soc. 132 (2010) 15839–15841.
[3] J. Snyder, T. Fujita, M.W. Chen, J. Erlebacher Nat. Mater. 9 (2010) 904–907.
[4] M. Lefevre, E. Proietti, F. Jaouen, J.P. Dodelet, Science 324 (2009) 71–74.
[5] K. Gong, F. Du, Z. Xia, M. Durstock, L. Dai, Science 323 (2009) 760–764.
[6] A. Kongkanand, S. Kuwabata, G. Girishkumar, P. Kamat, Langmuir 22 (2006) 2392–2396.
[7] J. Zhang, K. Sasaki, E. Sutter, R.R. Adzic, Science 315 (2007) 220–222.
[8] B. Lim, M.J. Jiang, P.H.C. Camargo, E.C. Cho, J. Tao, X.M. Lu, Y.M. Zhu, Y.N. Xia, Science 324 (2009) 1302–1305.
[9] F. Colmati, E. Antolini, E.R. Gonzalez, J. Power Sources 157 (2006) 98–103.
[10] J. Zhang, H.Z. Yang, J.Y. Fang, S.H. Zou, Nano Lett. 10 (2010) 638–644.
[11] W. Chen, J.M. Kim, S.H. Sun, S.W. Chen, J. Phys. Chem. C. 112 (2008) 3891–3898.
[12] W. Chen, S.W. Chen, Angew. Chem. 121 (2009) 4450–4453.
[13] Y.Y. Shao, J. Liu, Y. Wang, Y.H. Lin, J. Mater. Chem. 19 (2009) 46–59.
[14] R. Bashyam, P. Zelenay, Nature 443 (2006) 63–66.
[15] C.W.B. Bezerra, L. Zhang, K.C. Lee, H.S. Liu, A.L.B. Marques, E.P. Marques, H.J. Wang, J.J. Zhang, Electrochim. Acta 53 (2008) 4937–4951.
[16] Y. Tang, B.L. Allen, D.R. Kauffman, A. Star, J. Am. Chem. Soc. 131 (2009) 13200–13201.
[17] T. Iwazaki, R. Obinata, W. Sugimoto, Y. Takasu, Electrochem. Commun. 11 (2009) 376–378.
[18] E.J. Biddinger, D.V. Deak, U.S. Ozkan, Top. Catal. 52 (2009) 1566–1574.
[19] K.A. Kurak, A.B. Anderson, J. Phys. Chem. C. 113 (2009) 6730–6734.
[20] H. Niwa, K. Horiba, Y. Harada, M. Oshima, T. Ikeda, K. Terakura, J. Ozaki, S. Miyata, J. Power Sources 187 (2009) 93–97.
[21] C.P. Deck, K. Vecchio, Carbon 43 (2005) 2608–2617.
[22] L.P. Biro, Z.E. Horváth, A.A. Koos, Z. Osvath, Z. Vertesy, Al. Darabont, K. Kertesz, C. Neamtu, Zs. Sarkozi, L. Tapaszto, J. Optoelectron. Adv. Mater. 5 (2003) 661–666.
[23] C.P. Deck, G.S.B. McKee, K. Vecchio, J. Electron. Mater. 35 (2006) 211–222.
[24] B.L. Allen, P.D. Kichambare, A. Star, Nano Lett. 9 (2008) 1914–1920.
[25] J.W. Jang, C.E. Lee, S.C. Lyu, T.J. Lee, C.J. Lee, Appl. Phys. Lett. 85 (2004) 2877–2879.
[26] L. Qu, Y. Liu, J.B. Baek, L. Dai, Nano Lett. 4 (2010) 1321–1326.
[27] J. Liu, R. Czerw, D.L. Carroll, J. Mater. Res. 20 (2005) 538–543.
[28] K. Ghosh, M. Kumar, T. Maruyama, Y. Ando, Carbon 47 (2009) 1565–1575.
[29] Q.H. Yang, P.X. Hou, M. Unno, S. Yamauchi, R. Saito, T. Kyotani, Nano Lett. 5 (2005) 2465–2469.